第 48 卷 第 13 期/2021 年 7 月/中国激光 研究论文

中国激光

微透镜阵列结构膜提高 $CsPbBr_3$ 量子点薄膜发光效率及其稳定性

陈长锋[1,2]，郑懿[1]，方朝龙[2*]

[1]上饶幼儿师范高等专科学校，江西 上饶，334000；

[2]温州大学电气与电子工程学院微纳光电器件重点实验室，浙江 温州 325035

摘要 卤族钙钛矿量子点暴露在空气中，其发光效率通常很难保持稳定。本文采用磁力搅拌的方法把溴化铅铯量子点掺入到柔性微透镜阵列聚二甲基硅氧烷(PDMS)膜中，显著提高了溴化铅铯量子点的稳定性。实验研究发现制备的溴化铅铯量子点 PDMS 膜浸泡在水中和反复拉伸 1000 次其发光效率不下降。重要的是在 PDMS 表面引入微透镜阵列结构，发现微透镜阵列能够显著提高溴化铅铯量子点 PDMS 膜的发光效率和疏水性。这种柔性微透镜阵列量子点 PDMS 膜有望用于柔性 LED 中提高器件的发光效率和疏水性。

关键词 微纳光学；钙钛矿量子点；微透镜阵列；发光效率；疏水性

中图分类号 TN383 **文献标志码** A **doi**：10.3788/CJL202148.1313001

1 引 言

无机卤族钙钛矿量子点(QDs)拥有新颖的电学和光学性能，在最近几年已经引起了许多研究者的广泛关注[1-3]。这类无机卤族钙钛矿量子点已经广泛地用于光电二极管(LED)[4-5]、光学显示[6]、激光器[7]以及光发射[8]。尤其是其用于 LED 和光学显示时具有许多特别的优势，例如通过改变量子点的卤族元素其发光能覆盖整个可见光谱，从而可以通过替换卤族元素实现发光颜色的调谐[4,9]。除此之外卤族无机钙钛矿量子点拥有窄带宽、高量子产率，以及与稀土离子掺杂的荧光材料相比拥有低温的制备工艺等优点[10]。

尽管拥有上述优点，但稳定性差限制了它们的实际应用，例如无机卤族钙钛矿量子点暴露在空气中，由于空气湿度其发光性能会迅速衰减[11-12]。为了克服这个问题，研究者把卤族钙钛矿量子点封装在玻璃、聚合物膜以及石英颗粒中[9-10,12-14]。这种方法能有效阻隔量子点与空气中的水蒸气接触从而提高其稳定性。但是把钙钛矿量子点植入到玻璃中通常需要高温热处理。而把量子点掺入到聚合物中通常需要繁琐的制备流程，如在有机溶剂中超饱和结晶或者热注入、重复地离心、再在甲苯或者正己烷中均匀弥散，以及量子点与聚合物合成等[6,10,12]。因此从实际应用出发，发展一种简单制备拥有稳定性的量子点复合膜至关重要。与此同时，近几年发展的可穿戴电子产品、柔性 LED、柔性光展示已经获得了越来越广泛的关注，而柔性的卤族钙钛矿量子点复合物膜可以作为上述柔性器件的重要选择[15-17]。

尽管掺杂卤素钙钛矿量子点膜能够阻隔空气中的水蒸气提高量子点的稳定性，但是在材料与空气界面处有一个明显的折射率差，根据菲涅耳透射、反射系数，量子点的发出光在界面处发生反射或者全反射，限制了光的输出，进而会降低发光材料的发光效率，导致整个器件性能的下降。在材料界面引入

收稿日期：2020-11-10；**修回日期**：2020-12-03；**录用日期**：2021-01-11

基金项目：国家自然科学基金(61805179，61905180)、浙江省自然科学基金(LY19F050013)、江西省教育厅科学技术研究项目(GJJ191254)

通信作者：*fansy21@163.com

微透镜阵列结构减反膜能够有效地压制光反射，提高光输出已经被报道[18-20]。尤其是微透镜阵列结构应用到 LED 器件上，不仅提高 LED 器件发光效率，而且实现了 LED 的宽场照明与照明雾度值[21-22]。但是把微透镜阵列并入到发光膜上，研究微透镜阵列对其发光性能的影响少有报道。

本文提出了使用磁力搅拌方法把溴化铅铯钙钛矿量子点掺入到单组份的聚二甲基硅氧烷(PDMS)中，轻松制备了柔性溴化铅铯钙钛矿量子点 PDMS 膜。这种膜具有发光效率高、长时间浸没在水中或者重复拉伸变形发光效率不下降等优点。进而，理论和实验对比分析有无微透镜阵列结构时，量子点膜的发光效率。研究发现微透镜阵列结构能够有效提高量子点膜的发光效率。此外，我们测量了膜的表面疏水性，微透镜阵列结构也能够有效提高膜表面的水的接触角。

2 样品制备

样品的制备过程分为两个部分：溴化铅铯量子点 PDMS 溶液的制备和溴化铅铯量子点 PDMS 膜的制备。

1) 溴化铅铯量子点 PDMS 溶液的制备。溴化铅铯量子点 PDMS 溶液的制备过程如图 1 所示，它分为四个步骤：合成溴化铅铯量子点，混合溴化铅铯量子点正己烷溶液与 PDMS 预聚体，加入 PDMS 交联剂并充分搅拌，以及真空去除正己烷与气泡。

图 1(a)为溴化铅铯量子点的合成。①合成油酸铯盐溶液。首先将 40 mL 十八烯溶液倒入到三颈烧瓶中，再将 0.814 g 碳酸铯粉末倒入到十八烯溶液中，再将油酸溶液滴入到三颈烧瓶中。使用磁力搅拌器加热 120 ℃并充分搅拌至溶液清澈透明。随后将温度降至 100 ℃并保持。②合成油酸铅盐溶液。首先将 5 mL 十八烯溶液倒入到三颈烧瓶中，然后将 0.069 g 溴化铅粉末加入到三颈烧瓶中，使用磁力搅拌加热至 120 ℃。分别量取 0.5 mL 油胺溶液和 0.5 mL 油酸溶液滴入三颈烧瓶中并充分搅拌至溶液清澈透明。③合成溴化铅铯量子点。将油酸铅盐溶液升温至 150 ℃，再将 0.4 mL铯油酸盐溶液加入到油酸铅盐溶液中，随后迅速将三颈烧瓶放入到冰水中使其反应结晶形成溴化铅铯量子点。最后使用 5 mL 离心管离心取其沉淀物，使用正己烷溶解量子点，如此反复三次获得溴化铅铯量子点正己烷溶液。

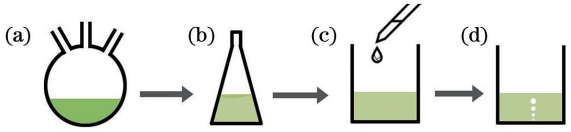

图 1 量子点 PDMS 溶液制备流程图

Fig. 1 Schematic diagram of PDMS solution preparation procedure

图 1(b)为混合量子点溴化铅铯正己烷溶液与 PDMS 预聚体。将溴化铅铯量子点正己烷溶液倒入称量好的 PDMS 预聚体中，超声振荡。图 1(c)为加入 PDMS 预聚体交联剂。将 PDMS 预聚体的交联剂(其质量大约为称量的 PDMS 预聚体的 0.1)滴入到 PDMS 与量子点正己烷的混合物中，并充分搅拌至均匀。为了判断其均匀性，将溶液在洁净的玻璃片上旋涂成膜，采用 365 nm 的紫光照明，薄膜中的量子点被激发，发射荧光。如果薄膜各个位置的荧光亮度无明显差异，可判断溶液配制均匀。图 1(d)为去除正己烷与气泡。在真空状态下，正己烷的沸点进一步降低，可以加速正己烷在常温下的挥发，并在真空下把搅拌过程中产生的气泡给去除。需要说明的是，在制备过程中，以 QD-x 形式标定相同 PDMS 预聚体的质量(1 g)、不同体积的溴化铅铯量子点正己烷溶液(x 表示量子点正己烷溶液的体积)混合的溴化铅铯量子点 PDMS 溶液。

2) 溴化铅铯量子点 PDMS 膜的制备。溴化铅铯量子点 PDMS 膜的制备如图 2 所示。图 2(a)为采用激光直写技术制备出微柱阵列。图 2(b)为热回流技术制备微透镜阵列[23-25]。使用热回流技术将微柱熔化，液态的光刻胶由于表面张力作用，在镀铬的石英基底表面形成接近于球面的液滴，再常温冷却形成微透镜阵列。图 2(c)为复制微透镜阵列结构。PDMS 预聚体与其交联剂以质量 10∶1混合，玻璃棒均匀后倒入到微透镜阵列结构后抽真空去气泡，加热固化后剥离形成凹的微透镜阵列结构。图 2(d)为表面改性。把 PDMS 凹的微透镜阵列放入到等离子清洗机中表面处理，使其表面改性。改性后放入到乙醇中浸泡 2 h，让其表面活跃层惰化。图 2(e)为复制获得凸的微透镜阵列结构。把第一部分获得的溴化铅铯量子点PDMS溶液倒入到凹

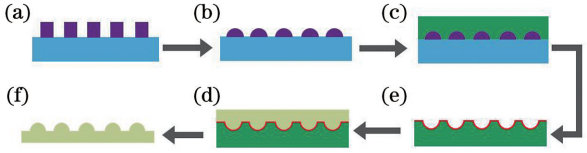

图 2 微透镜阵列溴化铅铯量子点 PDMS 膜的制备流程图

Fig. 2 Preparation procedure diagram of microlens-array PDMS coating with $CsPbBr_3$ QDs

的 PDMS 的微透镜阵列结构表面，加热固化获得凸的溴化铅铯量子点微透镜阵列结构膜，如图 2(f)所示。

3 分析与讨论

为了测试溴化铅铯量子点浓度对溴化铅铯量子点 PDMS 膜荧光强度的影响，本文测试了不同体积的溴化铅铯量子点溶液制备的量子点 PDMS 膜的荧光强度。在测试过程中使用 365 nm 光激发，接收光谱范围为 400～700 nm。图 3 为不同的掺杂浓度下荧光光谱图。初始 PDMS 膜的荧光强度随着浓度增加逐渐增大，随后浓度增加呈现下降的趋势。这个解释如下：首先溴化铅铯量子点浓度较低，荧光较低。当量子点浓度增加时，量子点发射的荧光逐渐累积，荧光增强。但是随着溴化铅铯量子点浓度增加，量子点的团聚效应也会增强，其直接的结果是量子点的颗粒增加，发光效率下降。这与参考文献[14]得到的结果一致。由图 3 可知，2.5 mL 溴化铅铯量子点正己烷溶液与 1 gPDMS 混合后获得荧光强度最强。因此选择标记 QD-2.5 mL 的溴化铅铯量子点 PDMS 溶液作为接下来的样品制备的依据。

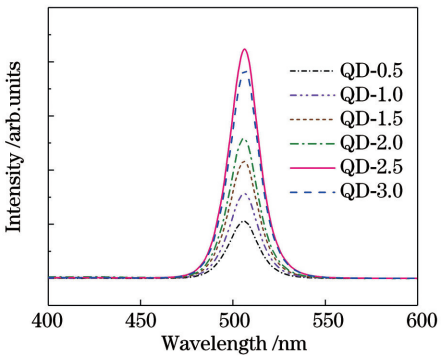

图 3 不同量子点浓度的 PDMS 膜荧光光谱图

Fig. 3 Fluorescence spectra of PDMS films with different quantum dot concentrations

为了评估溴化铅铯量子点 PDMS 膜用于 LED、光学显示等柔性器件的可行性，本文对制备的膜做了反复弯曲后的光致发光(PL)变化测试。图 4 为该膜在反复弯曲 1000 次后荧光强度变化。需要说明的是，每次弯曲的范围为 0°～180°，测量的所有光强都除以初始没有经过弯曲时的发光光强。从图 4 可以看出，每弯曲 100 次后其光致发光强度基本与没有弯曲之前相等，有力证明了该膜具有强柔韧性，并且在反复弯曲下其发光是非常稳定的，说明这种发光膜非常适合柔性白光 LED 的绿光发光层。

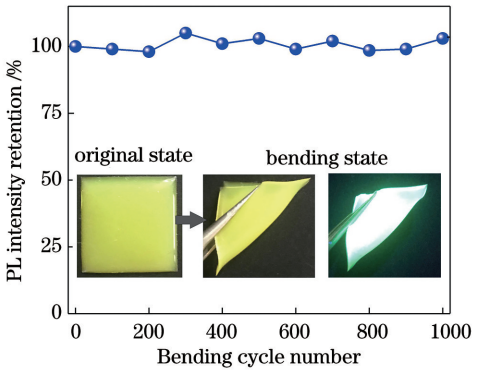

图 4 $CsPbBr_3$ 量子点 PDMS 膜弯曲次数与光致发光强度的关系(插图：膜的初始状态以及在弯曲状态下白光和 365 nm 光照下的照片)

Fig. 4 Relationship between the photoluminescence intensity and the bending times of the PDMS films(inset: initial state of the film as well as photos under white light and 365 nm light in the bending state)

无机钙钛矿 $CsPbBr_3$ 量子点在空气中其光致发光效率严重衰减，因为钙钛矿量子点的水稳定性较差。本文测试了无机钙钛矿 $CsPbBr_3$ 量子点 PDMS 膜放在水中其光致发光的稳定性。图 5(a)为 $CsPbBr_3$ 量子点 PDMS 膜浸没在水中其发光效率与时间的关系，其光致发光强度呈现非规律的变化，并且在 10 天的时间里量子点 PDMS 膜发光强度变化非常小，意味着无机钙钛矿 $CsPbBr_3$ 量子点掺杂在 PDMS 膜中能有效地隔离与水的接触，提高了 $CsPbBr_3$ 量子点的稳定性。为了进一步分析证明量子点 PDMS 膜水的耐受性，我们测量了量子点 PDMS 膜没有浸入水中之前、浸入了 5 天和 10 天的发光光谱。图 5(b)显示其发光光谱基本保持重合，再一次证明了无机钙钛矿 $CsPbBr_3$ 量子点掺入到 PDMS 膜中提高了其水耐受性。

为了展示微透镜阵列结构对溴化铅铯量子点 PDMS 膜发光的影响，本文测量了有、无微透镜阵列结构的溴化铅铯量子点 PDMS 膜的荧光光谱，如图 6(a)所示。图 6(a)为波长 400～600 nm 范围内的荧光强度与最大荧光强度(无微透镜阵列结构的溴化铅铯量子点 PDMS 膜)的比值。带有微透镜阵列的量子点的 PDMS 膜的荧光强度大约是没有微透镜阵列的较平的量子点 PDMS 膜 1.1 倍。为了进一步展示荧光强度的差别，我们把带有溴化铅铯量子点微透镜阵列 PDMS 膜放入到 365 nm 的紫光灯下，发现中间带有微透镜阵列的部分[其放大的扫描电子显微镜(SEM)图如图6(b)所示]，其荧光强

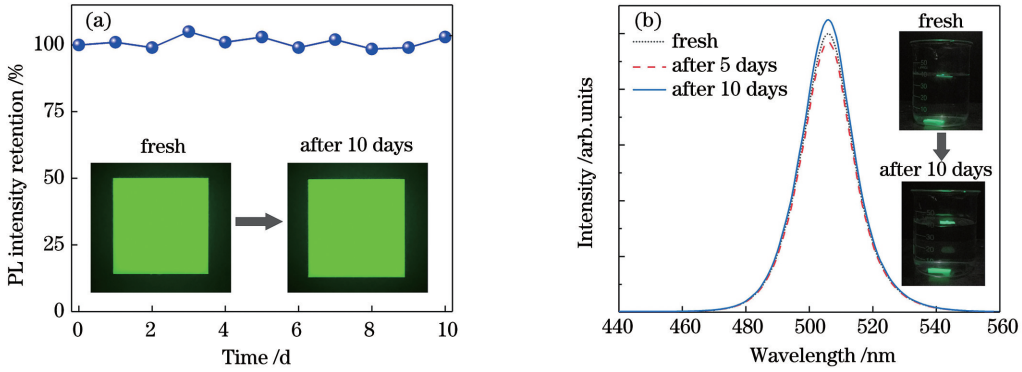

图 5　溴化铅铯量子点 PDMS 膜的水稳定性。(a)溴化铅铯量子点浸没在水中后，光致发光强度与时间的关系；(b)溴化铅铯量子点 PDMS 膜浸没在水中后光致发光光谱

Fig. 5　Water stability of PDMS films with $CsPbBr_3$ quantum dots. (a) Relationship between the photoluminescence intensity and the time after the PBCs QDs were immersed in water; (b) photoluminescence spectra of PBCs QDs PDMS films after immersion in water

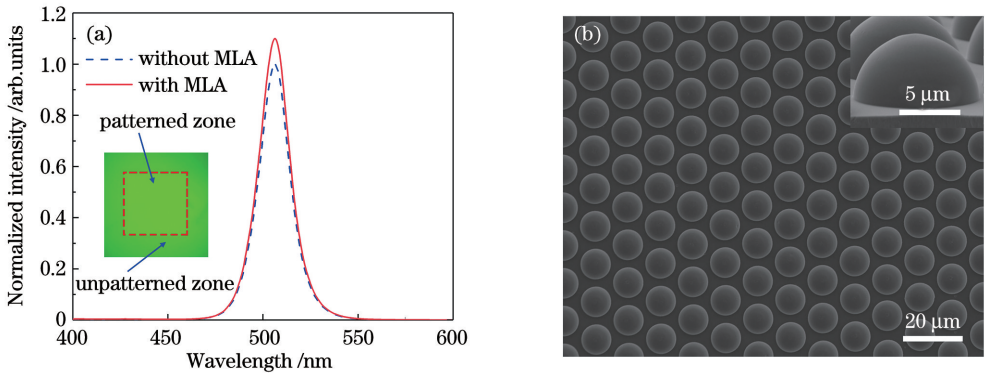

图 6　测量结果。(a)有无微透镜阵列结构的溴化铅铯量子点 PDMS 膜归一化光致发光光谱(插图：有无微透镜阵列图案溴化铅铯量子点 PDMS 膜发光对比照片)；(b)微透镜阵列 SEM 图

Fig. 6　Measurement results. (a) Normalized photoluminescence spectra of $CsPbBr_3$ quantum dots PDMS film with and without microlens array (inset: photo of $CsPbBr_3$ quantum dots PDMS film with or without microlens array pattern); (b) SEM image of microlens array

度明显高于没有图案的边缘区域，如图 6(a)插图所示。这个现象再一次证明了微透镜阵列结构能够有效提高溴化铅铯量子点的荧光输出。微透镜阵列结构提高荧光输出的现象主要是源于微透镜阵列结构能够减小光在空气-PDMS 界面反射，进而提高光的透过率。

为了解释这种现象，我们采用光线追踪方法模拟计算了光经过有、无微透镜阵列结构的 PDMS 膜光线的光程。在模拟计算中，本文设置光线能量小于最初光线的 1%将不被追踪，空气和 PDMS 折射率设置为 $n_{air}=1$ 和 $n_{PDMS}=1.41$。图 7 展示了三束光线以不同角度(0°，30°和 60°)穿过 PDMS-空气界面。图 7(a)显示三束光线从量子点溴化铅铯 PDMS 膜内发出到达微透镜阵列轮廓界面时，光线都能从界面传播到空气。与此相比，图 7(b)中三束

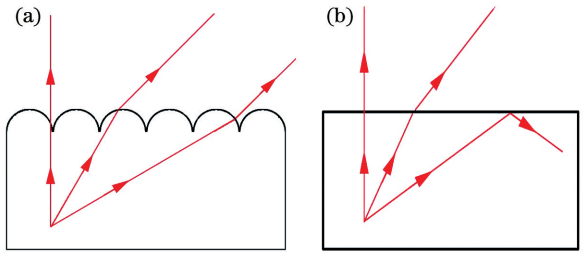

图 7　溴化铅铯量子点 PDMS 膜的在 $\theta=0°$，30°和 60°时光线追踪图。(a)微透镜阵列结构；(b)较平的溴化铅铯量子点 PDMS 膜

Fig. 7　Ray tracing diagram of the lead-cesium bromide quantum dot PDMS film at $\theta=0°$, 30°, and 60°. (a) Micro lens array structure; (b) flat lead-cesium bromide quantum dot PDMS film

光线传播到较平的界面时，由于光从光密到达光疏介质时，较大角度入射会发生全反射，全反射角度

可以通过全反射条件 $\theta=\arcsin(1/n_{\mathrm{PDMS}})=45.2°$ 获得。因此当光线入射角度达到 $\theta=60°$ 时，光线将不能有效传播到空气。这意味着在量子点 PDMS 膜表面引入微透镜阵列能有效避免量子点发出较大入射角的光线而发生全反射。其主要原因是微透镜阵列能够减小光的入射角度，避免发生全反射。另一方面，根据菲涅耳透射系数可知，减小入射角度可以增加光的透过率。因此引入微透镜阵列结构能够有效提高溴化铅铯量子点 PDMS 膜的发光效率。

此外本文还测量了有、无微透镜阵列结构的溴化铅铯量子点 PDMS 膜疏水性。图 8 显示了 2 μL 去离子水在有、无微透镜阵列结构的溴化铅铯量子点 PDMS 膜的状态。对于没有微透镜阵列结构的溴化铅铯量子点 PDMS 膜，水滴的接触角为 96.7°。与此相比，有微透镜阵列结构的溴化铅铯量子点 PDMS 膜其接触增大到 138.6°。实验结果证明了微透镜阵列结构还能够提高材料的表面的疏水性，预示着有微透镜阵列结构的溴化铅铯量子点 PDMS 膜在高湿度的环境中能够有效降低表面水的聚集，为该膜在高湿度环境中的应用奠定了基础。实际上，提高表面粗糙度能够有效提高材料表面的疏水性。这个可以解释如下：在较平的固体表面，三相接触线在铺展过程中不会遇到任何阻滞，液滴最终将达到其相应的热力学平衡态，呈现的（平衡）接触角也只由液体和固体表面的分子作用力的本质所决定，这样的接触角也称为杨氏接触角。而在粗糙表面，三相接触线在铺展过程中遇到粗糙结构的阻滞，使其无法跨越障碍、达到新的热力学平衡态，进而呈现较大的接触角。

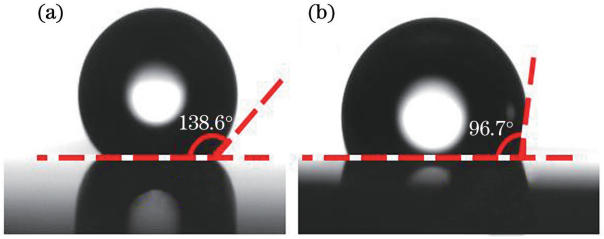

图 8 一个 2 μL 的去离子水在有无微透镜阵列结构的 PDMS 表面的形状。(a)水滴在 PDMS 微透镜阵列表面显示 138.6°接触角；(b)水滴在较平的 PDMS 表面显示了 96.7°的接触角

Fig. 8 Shape of a 2 μL deionized water on the surface of PDMS with or without microlens array structure. (a) Contact angle of water droplet on PDMS microlens array surface showing 138.6°; (b) contact angle of water droplet on flat PDMS surface showing 96.7°

4 结 论

本文利用化学合成制备了溴化铅铯无机钙钛矿溴化铅铯量子点，并将其掺杂到柔性的 PDMS 聚合物中获得量子点溴化铅铯 PDMS 膜。这种方法有效隔离无机钙钛矿溴化铅铯量子点与水的接触，提高了无机钙钛矿量子点的稳定性。重要的是在较平的溴化铅铯量子点 PDMS 膜表面引入微透镜阵列结构，理论和实验上都证明了微透镜阵列能够有效提高无机钙钛矿溴化铅铯量子点的发光效率。同时发现，微透镜阵列结构能有效提高溴化铅铯量子点 PDMS 膜表面的疏水性，为其在高湿度的环境应用奠定了基础。

参 考 文 献

[1] Protesescu L, Yakunin S, Bodnarchuk M I, et al. Nanocrystals of cesium lead halide perovskites ($CsPbX_3$, X = Cl, Br, and I): novel optoelectronic materials showing bright emission with wide color gamut[J]. Nano Letters, 2015, 15(6): 3692-3696.

[2] Wei K, Zheng X, Cheng X G, et al. Observation of ultrafast exciton-exciton annihilation in $CsPbBr_3$ quantum dots[J]. Advanced Optical Materials, 2016, 4(12): 1993-1997.

[3] Ai B, Liu C, Wang J, et al. Precipitation and optical properties of $CsPbBr_3$ quantum dots in phosphate glasses[J]. Journal of the American Ceramic Society, 2016, 99(9): 2875-2877.

[4] Li X M, Wu Y, Zhang S L, et al. Quantum dots: $CsPbX_3$ quantum dots for lighting and displays: room-temperature synthesis, photoluminescence superiorities, underlying origins and white light-emitting diodes[J]. Advanced Functional Materials, 2016, 26(15): 2435-2445.

[5] Li J H, Xu L M, Wang T, et al. 50-fold EQE improvement up to 6.27% of solution-processed all-inorganic perovskite $CsPbBr_3$ QLEDs via surface ligand density control[J]. Advanced Materials, 2017, 29(5): 1603885.

[6] Wang H C, Lin S Y, Tang A C, et al. Mesoporous silica particles integrated with all-inorganic $CsPbBr_3$ perovskite quantum-dot nanocomposites (MP-PQDs) with high stability and wide color gamut used for backlight display[J]. Angewandte Chemie, 2016, 55(28): 7924-7929.

[7] Wang Y, Li X M, Song J Z, et al. All-inorganic

colloidal perovskite quantum dots: a new class of lasing materials with favorable characteristics[J]. Advanced Materials, 2015, 27(44): 7101-7108.

[8] Hu F R, Zhang H C, Sun C, et al. Superior optical properties of perovskite nanocrystals as single photon emitters[J]. ACS Nano, 2015, 9(12): 12410-12416.

[9] Mao J, Lin H, Ye F, et al. All-perovskite emission architecture for white light-emitting diodes[J]. ACS Nano, 2018, 12(10): 10486-10492.

[10] Song Y H, Yoo J S, Kang B K, et al. Long-term stable stacked $CsPbBr_3$ quantum dot films for highly efficient white light generation in LEDs[J]. Nanoscale, 2016, 8(47): 19523-19526.

[11] Chen W W, Hao J Y, Hu W, et al. Optoelectronics: enhanced stability and tunable photoluminescence in perovskite $CsPbX_3$/ZnS quantum dot heterostructure[J]. Small, 2017, 13(21): 1604085.

[12] Park D H, Han J S, Kim W, et al. Facile synthesis of thermally stable $CsPbBr_3$ perovskite quantum dot-inorganic SiO_2 composites and their application to white light-emitting diodes with wide color gamut[J]. Dyes and Pigments, 2018, 149: 246-252.

[13] Wang Y W, Zhu Y H, Huang J F, et al. $CsPbBr_3$ perovskite quantum dots-based monolithic electrospun fiber membrane as an ultrastable and ultrasensitive fluorescent sensor in aqueous medium[J]. The Journal of Physical Chemistry Letters, 2016, 7(21): 4253-4258.

[14] Li Y, Lü Y, Guo Z Q, et al. One-step preparation of long-term stable and flexible $CsPbBr_3$ perovskite quantum dots/ethylene vinyl acetate copolymer composite films for white light-emitting diodes[J]. ACS Applied Materials & Interfaces, 2018, 10(18): 15888-15894.

[15] Dong L B, Xu C J, Li Y, et al. Flexible electrodes and supercapacitors for wearable energy storage: a review by category[J]. Journal of Materials Chemistry A, 2016, 4(13): 4659-4685.

[16] Li X Y, Liang R R, Tao J, et al. Flexible light emission diode arrays made of transferred Si microwires-ZnO nanofilm with piezo-phototronic effect enhanced lighting[J]. ACS Nano, 2017, 11(4): 3883-3889.

[17] Lee S Y, Park K I, Huh C, et al. Water-resistant flexible GaN LED on a liquid crystal polymer substrate for implantable biomedical applications[J]. Nano Energy, 2012, 1(1): 145-151.

[18] Eom S H, Wrzesniewski E, Xue J G. Close-packed hemispherical microlens arrays for light extraction enhancement in organic light-emitting devices[J]. Organic Electronics, 2011, 12(3): 472-476.

[19] Go H, Koh T W, Jung H, et al. Enhanced light-outcoupling in organic light-emitting diodes through a coated scattering layer based on porous polymer films[J]. Organic Electronics, 2017, 47: 117-125.

[20] Dong T T, Fu Y G, Chen C, et al. Study on bionic moth-eye antireflective cylindrical microstructure on germanium substrate[J]. Acta Optica Sinica, 2016, 36(5): 0522004.
董亭亭, 付跃刚, 陈驰, 等. 锗衬底表面圆柱形仿生蛾眼抗反射微结构的研制[J]. 光学学报, 2016, 36(5): 0522004.

[21] Kim A, Huseynova G, Lee J, et al. Enhancement of out-coupling efficiency of flexible organic light-emitting diodes fabricated on an MLA-patterned parylene substrate[J]. Organic Electronics, 2019, 71: 246-250.

[22] Leem Y C, Park J S, Kim J H, et al. Light-emitting diodes with hierarchical and multifunctional surface structures for high light extraction and an antifouling effect[J]. Small, 2016, 12(2): 161-168.

[23] Wang W, Zhou C H. New technology for fabrication of polymer microlens arrays[J]. Chinese Journal of Lasers, 2009, 36(11): 2869-2872.
王伟, 周常河. 一种新型聚合物微透镜阵列的制造技术[J]. 中国激光, 2009, 36(11): 2869-2872.

[24] Zhang X Y, Tang Q L, Zhang Z, et al. Concave refractive microlens arrays fabricated by ion beam etching[J]. Acta Optica Sinica, 2001, 21(4): 485-490.
张新宇, 汤庆乐, 张智, 等. 凹折射微透镜阵列的离子束刻蚀制作[J]. 光学学报, 2001, 21(4): 485-490.

[25] Liu X Y. Design of aspheric microlens made by photoresist reflow method[J]. Acta Optica Sinica, 2019, 39(2): 0208001.
刘向阳. 光刻胶热熔法制备的非球面微透镜的设计方法[J]. 光学学报, 2019, 39(2): 0208001.

Improvement of Luminescence Efficiency and Stability of $CsPbBr_3$ Quantum Dot Films with Microlens Array Structure

Chen Changfeng[1,2], Zheng Yi[1], Fang Chaolong[2*]

[1] *Continuing Education Center, Shangrao Normal College, Shangrao, Jiangxi* 334000, *China*;

[2] *Wenzhou Key Laboratory of Micro-Nano Optoelectronic Devices, College of Electrical and Electronic Engineering, Wengzhou University, Wenzhou, Zhejiang* 325035, *China*

Abstract

Objective Stable luminescent efficiency in inorganic halogen perovskite quantum dots (QDs) is difficult to achieve because of their degradation when exposed to air. In addition to stability, increased luminescence efficiency of QD composite films is an important factor for their future applications. Due to a sharp difference in refractive index between the air and flat QD film interface, some light is limited in the film, which has difficulty in crossing the interface and this decreases the luminescence efficiency of the QD film. This light is absorbed by the film and converted into thermal energy, which shortens the device's lifetime. Therefore, improvement of luminescence efficiency and stability of halogen perovskite QDs is essential. In this study, we report the fabrication of a flexible QD polydimethylsiloxane (PDMS) film with a microlens array (MLA) pattern using PDMS polymer mixed with lead cesium bromide ($CsPbBr_3$) QDs to transfer the concave MLA master mold. The flexible MLA QD film effectively improves luminescence efficiency and stability of the $CsPbBr_3$ QDs. Additionally, we find that introducing the MLA structure on the surface of the film significantly enhances surface hydrophobicity.

Methods The preparation procedure of $CsPbBr_3$ QD film with a MLA pattern is divided into the following two steps. (1) $CsPbBr_3$ QDs are synthesized by a conventional and simple chemical synthesis method and then dissolved into n-hexane (Fig. 1). Next, PDMS prepolymer and its crosslink agent are successively poured into the n-hexane QD solution in a weight ratio of 10∶1, and the solution is ultrasonically oscillated for uniformity. Finally, the $CsPbBr_3$ QD PDMS system is obtained by removal of n-hexane using vacuum. During the preparation process, both PDMS and its crosslink agent, with a constant weight of 1.1 g, are added into the $CsPbBr_3$ QD n-hexane solution in different volumes. The volume of $CsPbBr_3$ n-hexane solution is denoted by x (in mL) and the corresponding QD film is denoted as QD-x. (2) The second step of the preparation procedure is the transfer of the microlens array structure onto the surface of the $CsPbBr_3$ QD film (Fig. 2). First, a micropillar array is prepared by the laser direct writing technique and then the array is heated to melt and cooled to form a convex MLA master mold. Next, the convex MLA master mold is transferred onto the PDMS surface to form a concave MLA pattern using a soft lithography technique. The PDMS MLA pattern surface is modified by a plasma surface treatment and then immersed into ethyl alcohol for 4 h. Third, the $CsPbBr_3$ QD PDMS solution is poured onto the modified PDMS concave MLA surface, which is then followed by a degassing and curing process. Finally, a $CsPbBr_3$ QD film with the MLA pattern is obtained by separation from the PDMS concave MLA surface.

Results and Discussions The luminescence efficiencies of the prepared $CsPbBr_3$ QD films are measured using a fluorescence spectrometer (Fig. 3). With the increase of QD concentration, the number of QDs per unit volume of PDMS becomes large and the luminescence intensity of the QD film increases. However, the increase of QD concentration also increases the agglomeration of the QDs, which decreases the luminescence efficiency. In this experiment, QD-2.5 displays an optimum luminescence intensity and, thus, the QD PDMS system of QD-2.5 is selected as the prepared material for subsequent QD PDMS film fabrication. Moreover, this film displays stable luminescence intensity when repeatedly bent a thousand times or when immersed into water for ten days (Figs. 4 and 5). This demonstrates that the QD film is water-repellent and suitable for wearable flexible devices. The prepared MLA QD film shows about 10% increase in luminescence intensity compared to a flat QD film without any patterns (Fig. 6). This is mainly due to the antireflective property of the MLA pattern, which effectively avoids total reflection and decreases Fresnel reflection at the interface of air and the QD film (Fig. 7). When a 2 μL deionized water droplet is dropped on the surface of the prepared MLA QD film, the droplet shows a contact angle of 138.6°. By contrast, the contact angle is 96.7° when a 2 μL droplet is dropped on a flat QD film. The MLA pattern blocks the spreading of the water droplet and the three-phase contact line does not cross the obstacle, reaching a new thermodynamic equilibrium state. As a result, the droplet on the MLA pattern has a large contact angle. On a flat

solid surface, the three-phase contact line will not encounter any retardation. The droplet reaches its corresponding thermodynamic equilibrium state and thus displays a small contact angle. The experimental results demonstrate that the MLA QD film is suitable for high-humidity environment because its hydrophobic surface is not conducive to water vapor accumulation.

Conclusions Inorganic $CsPbBr_3$ QDs were synthesized by a conventional and simple chemical synthesis method. The synthesized CsPbBr QDs were uniformly added to PDMS by ultrasonic mixing, which was followed by removal of the n-hexane in the QD solution by vacuum. The PDMS QD film shows good luminescence stability under repeated bending or after immersion into water. After introducing the MLA pattern on the surface of the flexible QD film, the luminescence efficiency and surface hydrophobicity are significantly improved.

Key words micro-nano optics; perovskite quantum dot; microlens array; luminescence efficiency; hydrophobicity

OCIS codes 160.4670; 040.1240; 170.6280